Memoirs of the Scientific Sections of the Romanian Academy
Tome XLII, 2019

MATHEMATICS

A SURVEY OF NON-LINEAR PDE-BASED STRUCTURAL IMAGE INTERPOLATION MODELS

TUDOR BARBU

Institute of Computer Science of the Romanian Academy
E-mail: tudor.barbu@iit.academiaromana-is.ro

An overview of nonlinear partial differential equation (PDE)-based structural inpainting approaches is provided in this paper. The main image interpolation techniques based on variational models are described first. Next, the state of the art inpainting methods using PDE models of various orders that do not follow variational principles are presented. Some of our own contributions in this domain, representing variational and PDE-based inpainting algorithms, are also briefly described in this work.

Keywords: structure-based inpainting, nonlinear PDE model, variational scheme, anisotropic diffusion, high-order PDE, numerical approximation algorithm

1. INTRODUCTION

The image *interpolation* (*completion*) process aims at reconstructing the missing or highly deteriorated areas of the image as plausibly as possible, by using the image information achieved from the known surrounding regions. Another widely used term for this domain is *inpainting*, which has the origin in ancient art restoration [1]. The inpainting field has many important applications, such as: damaged digital artwork reconstruction, photo and movie renovation, undesired object removal, image super-resolution and zooming, and image decompression.

The interpolation techniques can be divided into three categories: texture-based inpainting, structure-based inpainting and combined approaches. While some textural interpolation methods are related to the texture synthesis [2], being inspired by influential texture synthesis algorithm of Efros and Leung [3], others represent exemplar-based techniques [4].

Structural inpainting approaches employ information around the missing part to estimate isophote from coarse to fine, and to diffuse the information by a diffusion mechanism. They reconstruct that missing part of the image by using variational and PDE models [5].

The state of the art energy-based, or variational, image interpolation techniques are described in the next section. The most important PDE-based inpainting approaches are presented in the third section.

We have conducted a high amount of research in the structure-based inpainting domain, developing numerous variational and nonlinear diffusion-based reconstruction techniques [6-9]. Our main contributions to the PDE-based inpainting field are also presented in the following two sections of the article. The paper ends with a section of conclusions and a list of references.

2. ENERGY-BASED STRUCTURAL INPAINTING TECHNIQUES

Variational (energy-based) structure-based interpolation methods complete the image affected by missing part by solving the minimization of an energy functional:

$$\min_u \left(E(u) = R(u) + \frac{1}{2}\int_\Omega \lambda_D (u - u_0)^2 \, d\Omega \right) \tag{1}$$

where the image domain $\Omega \subseteq R^2$, D is the inpainting domain, the *inpainting mask* is given by $\lambda_D = \lambda \cdot 1_{\Omega \setminus D}$, $\lambda > 0$ and u_0 is the observed image. While minimization of the *regularizing term R* (*u*), which contains certain a-priori information from the evolving image, is responsible for the filling process, the *fidelity term* $\frac{1}{2}\int_\Omega \lambda_D (u - u_0)^2 \, d\Omega$ forces the minimizer u to remain close enough to u_0 outside the inpainting domain [5].

Various inpainting models can be obtained, depending on the regularizer function. So, the Harmonic Inpainting is achieved by considering the regularizer $R(u) = \int_\Omega \|\nabla u\|^2 \, dxdy$ [1].

This simple variational inpaiting scheme cannot satisfy the *connectivity principle*, since it does not interpolate properly along the image gaps, and also produces too smooth results.

Some early variational image interpolation techniques were based on the Mumford-Shah segmentation model. Such an inpainting model uses the Γ - convergence approximation of the Mumford-Shah functional, of Ambrosio and Tortorelli [10], being characterized by the minimization:

$$\min_u \left(\frac{1}{2}\int_\Omega \lambda_D (u - u_0)^2 \, d\Omega + \frac{\gamma}{2}\int_{\Omega\setminus\Gamma} z_\in^2 |\nabla u|^2 \, d\Omega + \alpha \int_\Omega \left(\in |\nabla z_\in|^2 + \frac{(1 - z_\in)^2}{4 \in} \right) d\Omega \right) \tag{2}$$

where $z_{\in}$ is the signature function of the edge set. The inpainting algorithm based on (2) has a low order of complexity in terms of approximation and computation and a fast numerical convergence. It also preserves the sharpness of the boundaries very well.

An influential variational inpainting approach is Total Variation (TV) Inpainting elaborated by T. Chan and J. Shen in 2001 [11]. It is given by the following minimization:

$$\min_{u \in L^2(\Omega)} \left(E[u] = \int_{\Omega} \alpha \, \|\nabla u\| \, dx\,dy + \frac{\lambda_D}{2} \int_{\Omega} (u - u_0)^2 \, dx\,dy \right) \quad (3)$$

where $\alpha > 0$ and $\lambda_D = \lambda \cdot (1 - 1_D)$.

TV Inpainting reconstructs the missing part by minimizing the first-order total variation while remaining close to the initial image in the known zones. If a low value for α is selected, then smoothing is directed mainly to the inpainting domain. A second-order nonlinear anisotropic diffusion model is derived from (3), applying the Euler-Lagrange equation and the steepest gradient descent method:

$$\begin{cases} \dfrac{\partial u}{\partial t} = \alpha \, div \left(\dfrac{\nabla u}{|\nabla u|} \right) - \lambda_D (u - u_0) \\ u(0, x, y) = u_0 \end{cases}.$$

It works successfully and achieves connectivity, but not for large image gaps. Also, the TV Inpainting scheme is closely related to the TV Denoising model [ ], being derived from it by adding the inpainting mask.

Total variation based inpainting techniques of higher orders have been also developed in the last decades. Thus, the TV^2 Inpainting model is obtained by considering the second-order total variation as a regularizer component: $R(u) = \int_{\Omega} |\nabla^2 u| dxdy$ [1,12]. It outperforms TV Inpainting, producing better interpolation results and achieving more natural inpainted images. Also, TV^2 Inpainting provides a much better connectivity, being able to interpolate properly along large gaps.

The first and second-order TV regularizations can be combined to get improved inpainting results. A combined TV + TV^2 Inpainting approach reconstructs the image affected by the missing zones using the following minimization [12]:

$$u^* = \arg\min_u \left(\frac{\lambda_D}{2} \int_{\Omega \setminus D} (u - u_0)^2 dxdy + \int_{\Omega} \alpha(x) |\nabla u| dxdy + \int_{\Omega} \beta(x) |\nabla^2 u| dxdy \right) \quad (4)$$

where $\alpha(x)$ and $\beta(x)$ are two properly constructed spatially varying functions that control the inpainting process. The combined method (4) provides

effective results, outperforming both TV and TV^2 Inpainting. It completes succesfully large inpainting domains, avoiding the creation of blocky structures. It is numerically solved using the Split Bregman method [12].

Total Generalized Variation (TGV), representing a generalized version of the total variation model, involving higher-order derivatives of u and successfully used for filtering, can be also applied for interpolation. Some TGV-based inpainting approaches have been proposed in [13,14]. Other improved TV-based completion methods are Blind Inpainting using l_0 and TV Regularization [15] and TV Inpainting with Primal-Dual Active Set [16].

An important higher-order variational reconstruction model is Euler's Elastica Inpainting introduced by Chan and Shen [17]. This inpainting scheme is derived from (1) by applying the following regularizer:

$$R(u) = \int_D w(u)\left(\alpha + \beta\left(\nabla \cdot \frac{\nabla u}{|\nabla u|}\right)^2\right)|\nabla u|dxdy \tag{5}$$

where parameters $\alpha, \beta > 0$ control the behavior of the inpainting scheme and $w(u)$ is a weighing function depending on the histogram of u.

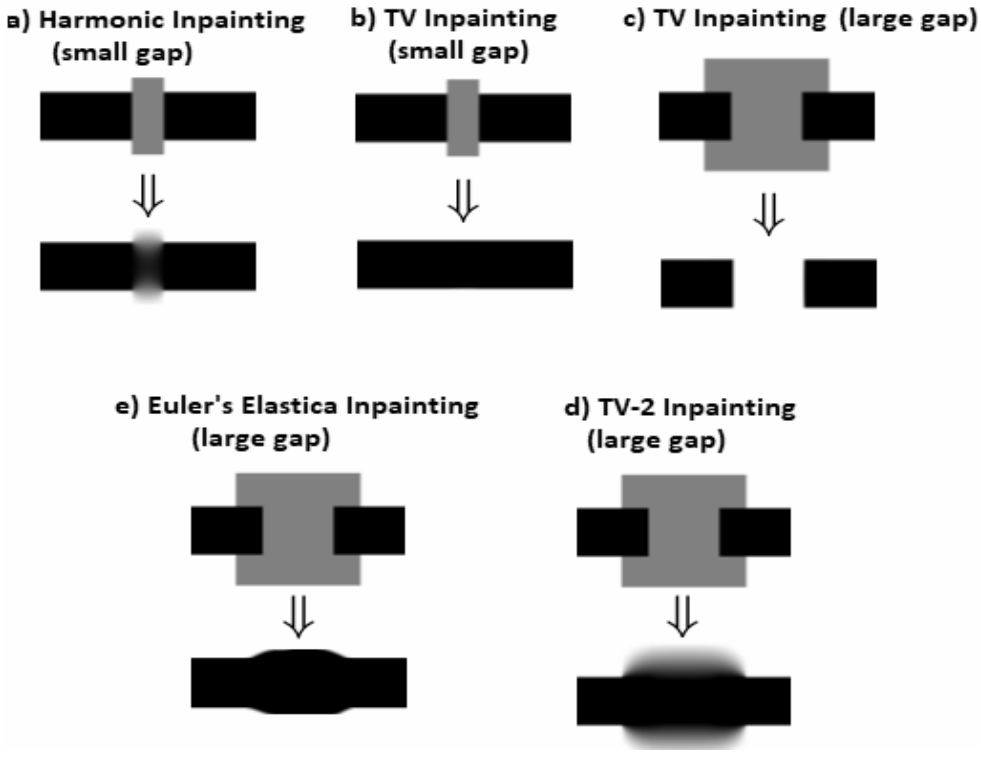

Fig. 1. Connectivity results provided by several variational inpainting models

Euler's Elastica Inpainting performs an effective image interpolation, being able to reconstruct large missing regions and working properly for noisy images. It provides a much better connectivity than TV Inpainting and other TV versions, being able to inpaint along much larger gaps.

Some inpainting examples related to several variational techniques are here described, as displayed in Figure 1. They aim to illustrate the connectivity power of these models.

We also developed numerous variational structural inpainting algorithms and disseminated them in several articles [6,7]. Let us now describe briefly a variational interpolation scheme proposed by us. It has a hybrid character, combining second and fourth order diffusions, as follows [7]:

$$u_{inp} = \arg\min_{u} \int_{\Omega} \phi_u^1 \left(\|\nabla u\| \right) + \phi_u^2 \left(|\Delta u| \right) + \frac{\alpha \left(1 - 1_{\Gamma}\right)}{2} \left(u - u_0\right)^2 d\Omega \quad (6)$$

where $\alpha, \lambda, \beta, \varepsilon \in (0,1]$, $\xi, \gamma \in [1,3]$, $k \in (0,4)$ and

$$\phi_u^1(s) = \int_0^s \tau\lambda \left(\frac{\eta_u}{\beta\tau^k + \xi} \right)^{\frac{1}{3}} d\tau; \phi_u^2(s) = \int_0^s \tau\xi \sqrt{\frac{\eta_u}{\varepsilon \log_{10}\left(\eta_u + \tau\right)^3 + \gamma}} d\tau \quad (7)$$

with the conductance parameter $\eta_u = \left| \nu\mu \left(\|\nabla u\| \right) - \zeta t \right|$, $\nu, \zeta \in (0,1)$.

The next fourth-order anisotropic diffusion model is derived from it:

$$\begin{cases} \dfrac{\partial u}{\partial t} = div\left(\delta_1^u \left(\|\nabla u\|\right)\nabla u\right) - \Delta\left(\delta_2^u \left(\left|\nabla^2 u\right|\right)\Delta u\right) - \alpha\left(1 - 1_{\Gamma}\right)\left(u - u_0\right) \\ u(t, x, y) = 0, \text{ on } \partial\Omega \setminus \Gamma \\ u(0, x, y) = u_0 \\ \dfrac{\partial u}{\partial \vec{n}} = 0 \end{cases} \quad (8)$$

Its solution, representing the inpainting result, is computed numerically using a consistent and fast-converging finite difference method based on an approximation algorithm [7]. Our technique provides a proper structural inpainting under both normal and noisy conditions. It preserves the edges and other details, and overcomes blurring and staircasing. Some method comparison results are provided in the next table and figure. Our approach outperforms many state of the art methods, achieving higher PSNR values [7].

Table 1. Average PSNR of various inpainting schemes

Inpainting method	**Average PSNR**
Proposed variational model	31.95 (dB)
TV Inpainting	29.96 (dB)
Harmonic Inpainting	27.32 (dB)
Mumford-Shah based Inpainting	30.27 (dB)
Bertalmio *et al*. model	31.75 (dB)

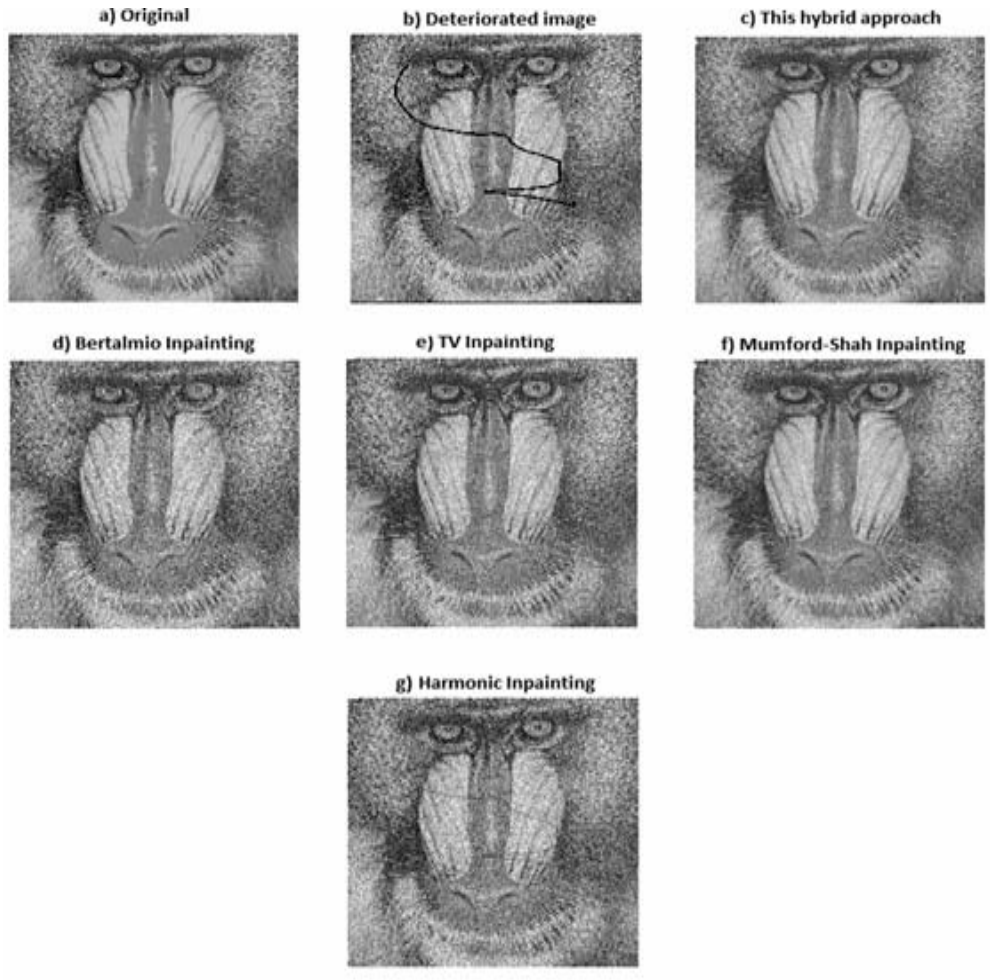

Fig. 2. *Mandrill* image inpainted by several reconstruction techniques

3. STATE OF THE ART NONLINEAR PDE-BASED INPAINTING TECHNIQUES

The partial differential equation-based structural inpainting models can be divided into two categories. The first one contains the nonlinear PDE models that follow variational principles, which means they can be derived from variational interpolation schemes like those described in the previous section.

A nonlinear second-order PDE inpainting model following variational principles is obtained by making the derivative of the energy functional at u equal to 0 and by applying the steepest descent method next. Thus, we have:

$$\frac{\partial u}{\partial t} + \nabla R(u) + \lambda_D (u - u_0) = 0 \text{ in } \Omega \tag{9}$$

Many second-order PDE-based inpainting methods have been developed in the last decades, using various selections of the regularizer term, $R(u)$. Also, the models given by (9) can be regarded as PDE-based denoising schemes adapted for interpolation by adding the inpainting mask.

The PDE inpainting models that do not follow variational principles are not derived from some minimization problems, being directly provided as evolutionary differential equations. They include some state of the art high-order PDE-based reconstruction algorithms.

The third order PDE-based inpainting technique proposed by Bertalmio, Sapiro, Ballester and Caselles is an influential approach in this field [18]. Their interpolation approach propagates the necesary information in the direction of the isophotes [18], being characterized by the third order PDE:

$$\frac{\partial u}{\partial t} = \nabla^{\perp} u \cdot \nabla \Delta u \tag{10}$$

where $\nabla^{\perp} u$ is the perpendicular gradient of u. This represents a transport equation for image smoothness, which is modeled by image's Laplacian along its level lines. The next PDE is obtained by introducing anisotropic diffusion to avoid the level-line crossing:

$$\frac{\partial u}{\partial t} = \nabla^{\perp} u \cdot \nabla \Delta u + \nabla \cdot \left(g\left(|\nabla u| \right) \nabla u \right) \tag{11}$$

where g is a properly selected smooth function. Its goal is to evolve the PDE to a steady-state solution, where $\nabla^{\perp} u \cdot \nabla \Delta u = 0$, ensuring that information is constant in isophotes' direction. This third-order PDE scheme aims at proving that both gradient direction and gray-scale values must be propagated inside the inpainting

domain, and shows why high-order PDE are required by a proper interpolation. A reconstruction example, representing an old photo inpainted by this approach, is displayed in the next figure [18].

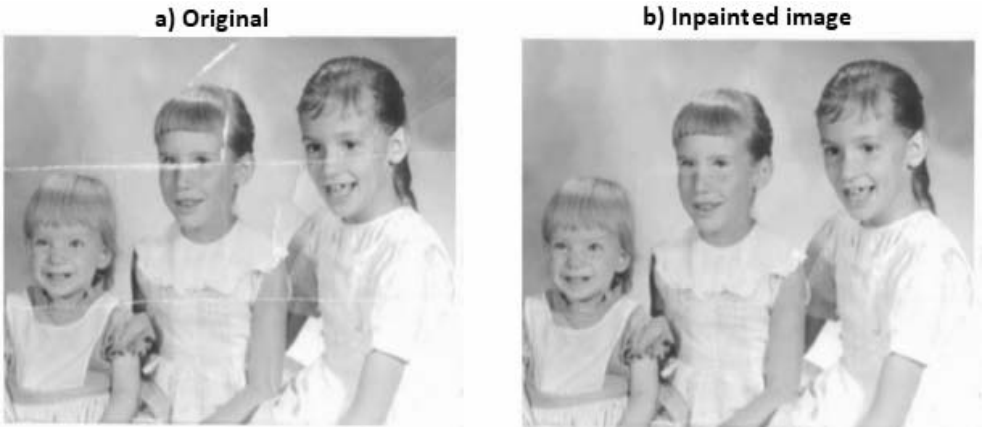

Fig. 3. Old photo reconstructed by Bertalmip et. al Inpainting

Another important third-order PDE-based structural inpainting method is Curvature-driven Diffusion (CDD) Inpainting, introduced by Chan and Shen [1,19], which fixes the drawbacks of their TV Inpainting algorithm by using the curvature information of the level lines. It has the form:

$$\begin{cases} \dfrac{\partial u}{\partial t} = \nabla \cdot \left(\dfrac{g(\kappa)}{|\nabla u|} \nabla u \right) - \lambda_D (u - u_0) \\ u(0, x, y) = u_0 \end{cases} \tag{12}$$

where the isophote curvature

$$\kappa = \nabla \cdot \left[\frac{\nabla u}{|[\nabla u]|} \right] \text{ and } g(s) = s^p,\ p \geq 1 \text{ [9].}$$

The CDD model diffuses the smoothness perpendicularly to the level lines, preserves their direction and is able to connect them across large distances. CDD Inpainting has its own drawbacks, one of them being the noise sensitive character.

The PDE in (12) is solved using a finite difference-based numerical approximation scheme described in [19]. Thus, the flux of the CDD model is computed as $j = -\dfrac{g(k)}{|\nabla u|}\nabla u$, so that equation (12) becomes $\dfrac{\partial u}{\partial t} = -\nabla \cdot j$ and is discretized using the explicit iterative algorithm:

$$u^{n+1} = u^n - \Delta t \left[\nabla \cdot j\right]^{(n)} \tag{13}$$

where $t = n\Delta t$ and $\left[\nabla \cdot j\right]^{(n)}$ is the discretization of divergence $\nabla \cdot j$, which is computed using the half-point central differences [19].

Many well-known inpainting tasks, such as disocclusions, old photo reconstruction, text and object removal are performed sucessfully using CDD Inpainting. A text removal example is displayed in Figure 4 [19].

Fig. 4. Text removal using CDD Inpainting

Some of the influential high-order PDE-based reconstruction techniques are based on nonlinear fourth-order PDE models. One of these approaches is the Cahn-Hilliard Inpainting model [1,20], which uses the next modified version of Cahn-Hilliard equation (a fidelity term being added) with Neumann boundary conditions:

$$\begin{cases} u_t = -\Delta\left(\varepsilon\Delta u - \frac{1}{\varepsilon}W'(u)\right) - \lambda(x,y)(u - u_0), in\ \Omega \\ \frac{\partial u}{\partial \nu} = \frac{\partial \Delta u}{\partial \nu} = 0, on\ \partial\Omega \end{cases} \tag{14}$$

where the nonlinear double-well potential function $W(u) = u^2(u-1)^2$ and $\lambda(x,y) = \begin{cases} \lambda_0 \geq 1, (x,y) \in \Omega \setminus D \\ 0, (x,y) \in D \end{cases}$.

The fourth-order Cahn-Hilliard model is well-posed, the global existence of a unique weak solution being proved in [20]. It is solved numerically by applying the *convexity splitting* fast solver [20].

Cahn-Hilliard Inpainting provides a smooth continuation of the level lines into the inpainting domain *D*, like CDD Inpainting, but it converges much faster

[20]. An example of object removal using Cahn-Hilliard Inpainting is displayed in Figure 5 [20].

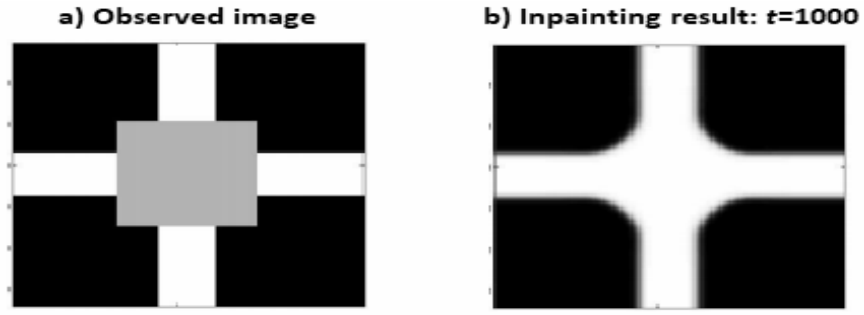

Fig. 5. Object removal using Cahn-Hilliard Inpainting

TV – H^{-1} Inpainting represents another important nonlinear fourth-order interpolation method [1,21]. It is given by equation:

$$u_t = \Delta p + \lambda(x, y)(u_0 - u),\ p \in \partial TV(u) \tag{15}$$

where $u_0 \in L^2(\Omega)$ and $\partial TV(u)$ represents the subdifferential of $TV(u) = \begin{cases} |Du|(\Omega), if\ |u| \le 1\ a.e.\ in\ \Omega \\ +\infty, otherwise \end{cases}$, $|Du|(\Omega)$ being the total variation of *u*.

The stationary equation $\Delta p + \lambda(u_0 - u) = 0$ admits a solution $u \in BV(\Omega)$ [21], which is computed numerically by applying the next time-stepping numerical approximation scheme:

$$\frac{U_{k+1} - U_k}{\Delta t} + C_1 \Delta\Delta U_{k+1} + C_2 U_{k+1} = C_1 \Delta\Delta U_k - \Delta\left(\nabla \cdot \left(\frac{\nabla U_k}{|\nabla U_k|_\in}\right)\right) + C_2 U_k + \lambda(u_0 - U_k) \tag{16}$$

where $C_1 > \frac{1}{\in}$ and $C_2 > \lambda_0$.

The TV – H^{-1} Inpainting scheme provides effective completion, outperforming the TV Inpainting model, but it requires a high number of iterations of the algorithm (16), given its complexity. See a TV – H^{-1} Inpainting example in the next figure.

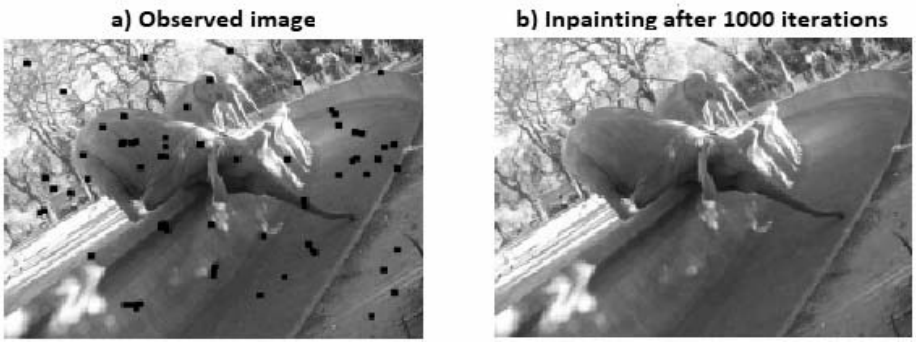

Fig. 6. TV - H^{-1} Inpainting: $\lambda_0 = 10^2, \epsilon = 0.01$

LCIS (*low curvature image simplifiers*) Inpainting is a nonlinear fourth-order PDE-based interpolation approach proposed in 1999 [22] and characterized by the next partial differential equation:

$$u_t = -\nabla \cdot \left(g\left(|\nabla u|\right)\nabla \Delta u\right) + \lambda\left(u_0 - u\right) \tag{17}$$

where $u_0 \in L^2(\Omega)$ and function $g(s) = \dfrac{1}{1+s^2}$.

Equation (17) leads to $u_t = -\nabla \cdot \left(\arctan\left(\Delta u\right)\right) + \lambda\left(u_0 - u\right)$.

The fourth-order LCIS model is solved numerically by using a convexity splitting approach [22]. Because of the complexity of its numerical approximation scheme, LCIS Inpainting does not execute fast, providing successful interpolation results after hundreds of iterations. Inpainting tasks such as text or object removal are performed effectively using the LCIS scheme.

We have elaborated many nonlinear parabolic and hyperbolic second and fourth order PDE models for structure-based inpainting in the last decade [6-9]. While most of them follow the variational principle [6,7], some cannot be derived from minimization problems [9].

An effective second-order PDE-based structural inpainting framework developed by us was disseminated in [9]. It is based on the following nonlinear anisotropic diffusion-based model:

$$\begin{cases} \dfrac{\partial u}{\partial t} - \psi^u\left(\|\nabla u\|\right)\nabla \cdot \left(\varphi_u\left(\|\nabla u\|\right)\nabla u\right) + \lambda\left(1 - 1_\Gamma\right)\left(u - u_0\right) = 0, \quad \forall (x,y) \in \Omega \\ u(x,y,0) = u_0(x,y), \quad \forall (x,y) \in \Omega \\ u(t,x,y) = 0, \quad \forall (x,y) \in \partial\Omega \end{cases} \tag{18}$$

where $\lambda \in (0,1]$, $\psi^u(s) = \gamma\left(\alpha s^r + \beta\right)^{\frac{1}{r+1}}$, $\alpha, \gamma \in (0,3], \beta \in (0,3.5]$ and $r \in (0,2]$.

Its diffusivity function has the form:

$$\varphi_u : [0,\infty) \to [0,\infty)$$

$$\varphi_u(s) = \delta\left(\frac{\eta(u)}{\xi s^k + \nu \log 10(\eta(u))}\right)^{\frac{1}{k+1}} \tag{19}$$

where $\delta \in (0,2)$, $\xi \in (1,5]$, $\nu \in (0,1)$, $k \in \{1,2,3,4\}$ and the conductance parameter

$$\eta(u(x, y, t)) = |\varepsilon\mu(\|\nabla u\|) + \zeta t|, \ \varepsilon > 1, \ \zeta \in (0,1).$$

This anisotropic diffusion model is well-posed, its mathematical validity being demonstrated in [9]. It admits a unique weak solution that is numerically computed using a finite difference-based numerical approximation scheme [23] which is stable and consistent to the PDE model (18) [9].

This second-order diffusion-based technique reconstructs successfully the image by directing diffusion to the inpainting domain while preserving their edges, corners and other details. Our method outperforms variational approaches like Harmonic and TV Inpainting, achieving better average MSE and PSNR values, and also comparable good results to some fourth-order PDE inpainting models, like TV – H^{-1} Inpainting [9]. Some method comparison results are listed in the next figure and table.

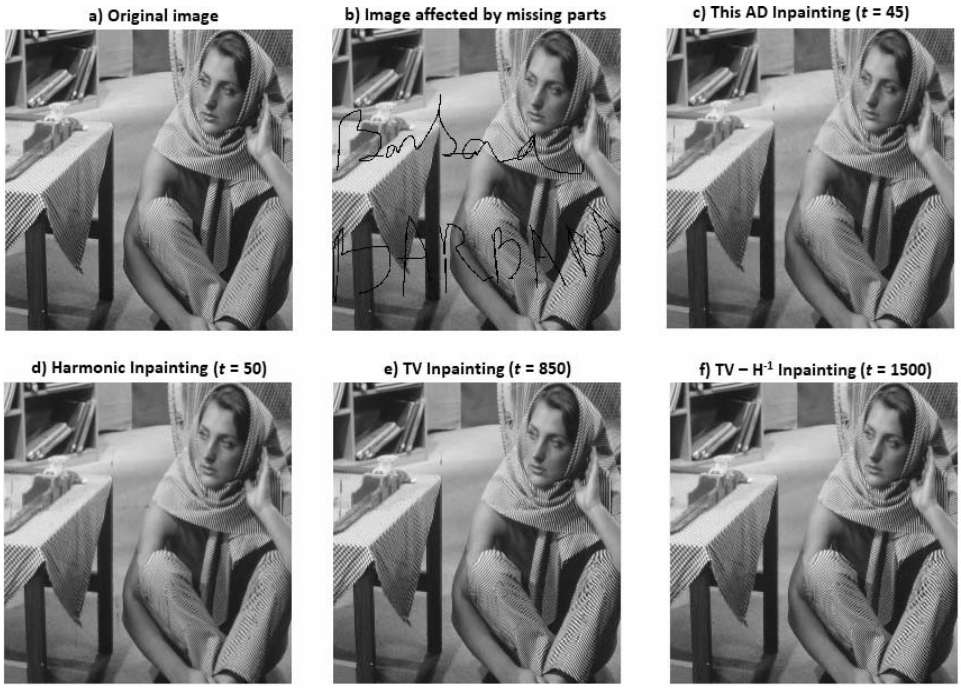

Fig. 7. Intpainting results of several PDE-based approaches

Table 2. Average PSNR and MSE values of several PDE inpainting models

Inpainting algorithm	Average PSNR	Average MSE
Proposed AD Inpainting	36.1338 (dB)	15.8380
Harmonic Inpainting	29.6887 (dB)	69.8576
Total Variation Inpainting	34.2561 (dB)	24.4047
TV – H^{-1} Inpainting	36.3805 (dB)	14.9634

4. CONCLUSIONS

A survey on the state of the art structural inpainting techniques using nonlinear PDE-based models has been provided here. Two categories of PDE interpolation schemes have been addressed in this work, our own contributions in each of them being disscused.

The state of the art variational interpolation approaches have been disscused first. They are closely related to the variational restoration models and can be easily derived from them by using an inpainting mask. Nonlinear PDE-based inpainting schemes could be derived from them. A variational image interpolation technique proposed by us, combining second- and fourth-order diffusions, has been presented.

State of the art PDE-based structural inpainting techniques not following variational principles have been described next. While the most important of these models have higher orders, some influential third- and fourth-order PDE models for image completion being described here, we developed a second-order nonlinear diffusion-based inpainting solution not following variational principles, which has been also presented.

The structural inpainting techniques proposed by us provide satisfactory reconstruction results, work succesfully in noisy conditions and avoid the undesired effects. They outperform many of the described state of the art structure-based inpainting methods, but, unfortunately, they do not work properly for image textures.

REFERENCES

1. SCHONLIEB, C. B. *Partial Differential Equation Methods for Image Inpainting*, Volume 29, Cambridge University Press, 2015.
2. IGEHY, H., PEREIRA, L. *Image replacement through texture synthesis*, Proceedings of the International Conference on Image Processing, 1997, 3, 186–189.
3. EFROS, A., LEUNG T. K., *Texture synthesis by non-parametric sampling*, Proceedings of the International Conference on Computer Vision, volume 2, 1999, 1033–1038.
4. CRIMINISI, A., PEREZ, P., TOYAMA, K. *Region filling and object removal by exemplar-based image inpainting*, IEEE Transactions on Image Processing, vol. 13, 2004, 9, 1200–1212.
5. SONG, B. *Topics in Variational PDE Image Segmentation, Inpainting and Denoising*, University of California, 2003.

6. BARBU, T. *Variational image inpainting technique based on nonlinear second-order diffusions*, Computers & Electrical Engineering, Volume 54, August 2016, 345–353.
7. BARBU, T. *Hybrid Image Interpolation Technique based on Nonlinear Second and Fourth-order Diffusions*, Proceedings of the 13th International Symposium on Signals, Circuits and Systems, ISSCS'17, Iasi, Romania, July 13–14, 2017, 1–5.
8. BARBU, T. *Structural Image Interpolation using a Nonlinear Second-order Hyperbolic PDE-based Model*, Proceedings of the 6th IEEE International Conference on e-Health and Bioengineering, EHB 2017, Sinaia, Romania, 22–24 June 2017, 5–8.
9. BARBU, T. *Second-order Anisotropic Diffusion-based Framework for Structural Inpainting*, Proceedings of the Romanian Academy, Series A: Mathematics, Physics, Technical Sciences, Information Science, Volume 19, Issue 2, April – June 2018, 329–336.
10. AMBROSIO, L., TORTORELLI, V. M. *Approximation of functionals depending on jumps by elliptic functionals via* Γ *- convergence*, Comm. Pure Appl. Math., 1990, 43, 999-1036.
11. CHAN, T. F., SHEN J., *Morphologically invariant PDE inpaintings*, UCLA CAM Report, 2001, 1–15.
12. PAPAFITSOROS K., SCHONLIEB, C. B., SENGUL B. *Combined first and second order total variation inpainting using split Bregman*, Image Process. On Line, Jan. 2013, 2013, 112–136.
13. BREDIES, K., HOLLER M. A *TGV-based framework for variational image decompression, zooming, and reconstruction*, Part I: Analytics, SIAM J. Imag. Sci., vol. 8, no. 4, 2015, 2814–2850.
14. BREDIES, K., HOLLER M. A *TGV-based framework for variational image decompression, zooming, and reconstruction*, Part II: Numerics, SIAM J. Imag. Sci., vol. 8, 2015, 4, 2851–2886.
15. AFONSO, M. V., SANCHES J. M. R., *Blind Inpainting Using l0 and Total Variation Regularization*, IEEE Transactions on Image Processing, 2015, 24 (7), 2239–2253.
16. NERI, M., ZARA E. R. *Total variation-based image inpainting and denoising using a primal-dual active set method*, Philippine Science Letters, Vol. 7, 2014, 1, 97–103.
17. CHAN T. F., KANG S.-H, SHEN J. *Euler's elastica and curvature based inpaintings*, SIAM J. Appl. Math., 2002.
18. BERTALMIO, M., SAPIRO. G., CASELLES V., BALLESTERS, C., *Image inpainting*, Proc. ACM Conf. Comp. Graphics (SIGGRAPH), New Orleans, LU, July 2000, 417–424.
19. CHAN T. F., SHEN J., *Non-texture inpainting by curvature-driven diffusions (CDD)*, J. Visual Comm. Image Rep., 2001, 4 (12), 436–449.
20. BURGER, M., HE, L. *Cahn-Hilliard inpainting and a generalization for grayvalue images*, SIAM J. Imaging Sci., 2009, 2 (4), 1129–1167.
21. OSHER, S., SOLE A., VESE, L., *Image decomposition and restoration using total variation minimization and the H-1 norm*, Multiscale Modeling and Simulation: A SIAM Interdisciplinary Journal, Vol. 1, 2003, 3, 349–370, 2003.
22. SCHONLIEB C. B., BERTOZZI, A. *Unconditionally stable schemes for higher order inpainting*, Comm. Math. Sci., vol. 2,2011, 9, 413–457.
23. JOHNSON, P., *Finite Difference for PDEs*, School of Mathematics, University of Manchester, Semester I, 2008.